JACS
JOURNAL OF THE AMERICAN CHEMICAL SOCIETY
Article
pubs.acs.org/JACS

Self-Assembly, Host–Guest Chemistry, and Photophysical Properties of Subphthalocyanine-Based Metallosupramolecular Capsules

Irene Sánchez-Molina,[†] Bruno Grimm,[‡] Rafael M. Krick Calderon,[‡] Christian G. Claessens,*[,†] Dirk M. Guldi,*[,‡] and Tomas Torres*[,†,§]

[†]Departamento de Química Orgánica, Universidad Autónoma de Madrid, 28049 Madrid, Spain
[‡]Department of Chemistry and Pharmacy and Interdisciplinary Center for Molecular Materials (ICMM), Friedrich-Alexander-Universität Erlangen-Nürnberg, 91058 Erlangen, Germany
[§]IMDEA-Nanociencia, c/Faraday, 9, Campus de Cantoblanco, 28049-Madrid, Spain

Supporting Information

ABSTRACT: Four new subphthalocyanine-based capsules have been synthesized and characterized. These supramolecular systems have been successfully employed for the encapsulation of fullerenes and probed by a wide range of characterization methods, including NMR, UV–vis and fluorescence spectroscopy, electrospray ionization mass spectrometry, and electrochemistry. Furthermore, the binding constants of the host guest complexes were estimated. Finally, the photophysical properties revealed that the subphthalocyanines undergo a transduction of singlet excited-state energy to the fullerene inside the cavity upon photoexcitation.

INTRODUCTION

Subphthalocyanines[1] (SubPcs) are 14 π-electron aromatic macrocycles containing three 1,3-diiminoisoindol units *N*-fused around a central boron atom. Their particular concave π-extended structure sets them as potential receptors of complementary convex-shaped molecules, such as fullerenes,[2] widely used in the field of molecular materials. Additionally, their remarkable electrochemical and photophysical properties render them interesting probes for studying light-induced processes.[3] In fact, covalently linked SubPc-C_{60} conjugates have been studied before, showing either energy- or electron-transfer processes. If C_{60} was attached to the axial position of the SubPc and, thus, close to its convex face, energy transfer occurred unless the periphery of the SubPc was substituted with donor groups.[4] However, when C_{60} was linked to the SubPc core in a way that it was exposed to the concave face of the macrocycle, distance was the decisive factor that determines if either electron or energy transfer takes place.[5]

Furthermore, fullerenes interact with the concave face of SubPcs by means of supramolecular interactions, owing to the shape complementarity of their aromatic surfaces. In a recently published study, the dependence of such interactions on the electronic nature of SubPc has been demonstrated. To this end, binding constants with values ranging from 10^4 to 10^5 M^{-1} have been reported. Photophysical studies performed by us allowed the observation of energy transfer occurring upon photoexcitation of the SubPc.[6] Moreover, supramolecular π–π stacking between SubPcs and C_{60} has also been observed by Ziessel et al. in solution[7a] and by Kobayashi et al. in the solid state.[7b]

On the other hand, coordination-driven self-assembly[8] has proved to be a powerful tool for obtaining not only structurally interesting 2D polygons or 3D polyhedra but also self-assembled species that are active as molecular containers, catalysts, molecular materials, etc. In this context, SubPcs arise as ideal building blocks for the construction of functional homodimeric capsules due to their curve-shaped structure and their synthetic versatility. Thus, the tritopic C_3-symmetric receptor **1** (Figure 1), which combines both the preorganization of the rigid SubPc skeleton and three pyridyl units, was self-assembled into a heterochiral cage of C_{3h} symmetry in the presence of stoichiometric amounts of $Pd(en)(NO_3)_2$. Remarkably, such a high degree of symmetry was found to be the result of chiral self-discrimination between the enantiomers of SubPc **1** during the self-assembling process.[9] The internal aromatic concave faces of a SubPc homodimeric metallosupramolecular capsule form an excellent system for probing π–π stacking interactions in the particular case of nonplanar molecules. Thus, a similar M_3L_2 SubPc capsule, obtained from SubPc **2** (Figure 1), in which extra triple bond spacers were added between the SubPc periphery and the 3-pyridyl unit, was shown to strongly interact with C_{60} in acetone solution, where C_{60} itself is insoluble.[10] These SubPc-based capsules were also

Received: April 28, 2013
Published: June 13, 2013

 © 2013 American Chemical Society dx.doi.org/10.1021/ja404234n | J. Am. Chem. Soc. 2013, 135, 10503–10511

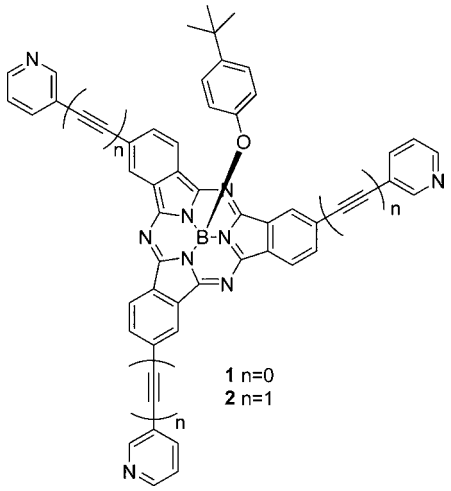

Figure 1. SubPcs **1** and **2**.

found to be excellent for the study of dynamic processes associated with the formation of metallosupramolecular assemblies.[11]

We describe herein the self-assembly of a series of four new M_3L_2 capsules based on SubPc **2**. Phosphines were chosen as ligands in order to allow quick characterization by ^{31}P NMR, and Pd (II) and Pt (II) were employed as coordinating centers. Both diphenylphosphinopropane and diphenylphosphinoferrocene were used as secondary ligands. The latter provides additional donors at the periphery of the system. These supramolecular containers were shown to form 1:1 adducts with C_{60}, C_{70}, and their soluble PCBM-type derivatives in dichloromethane. The $\pi-\pi$ interactions between the fullerenes and the SubPc walls of the capsules were quantified through determining the binding constants and the stoichiometry of the resulting adducts. Communication between the two complementary π-surfaces was also demonstrated by measuring photoinduced processes.

EXPERIMENTAL SECTION

Self-Assembly: Method A. A dichloromethane solution of stoichiometric amounts of SubPc **2** and the corresponding metal complex was stirred under argon and heated under reflux for different periods of time. After completion, the solution was concentrated, and diethylether was added. Finally, the resulting precipitate was filtered and washed sequentially with cold toluene, hexane, and diethylether.

Method B. SubPc **2** (0.006 mmol, 1 equiv) and C_{60} or C_{70}-PCBM (3.6×10^{-3} mmol, 1.2 equiv) were dissolved in 2.5 mL of dry dichloromethane and stirred under argon at room temperature for 1 h. Subsequently, the metal complex was added (0.009 mmol), and the mixture was refluxed for 18 h and then left to cool down to room temperature for 1 h. The solution was concentrated, and diethylether was added. Finally, the resulting precipitate was filtered and washed with cold toluene, hexane, and diethylether. If fullerene template remains, it can be eliminated by gel permeation chromatography (Bio Beads S-X1, 200–400 mesh).

SubPc 3. To 1g of 3-iodophthalonitrile, 1.6 mL of 1 M solution of BCl_3 in *p*-xylene was added under an argon atmosphere. The mixture was refluxed for 2 h, and then volatiles were eliminated with an argon stream. Subsequently, 350 mg of 4-*t*-butylphenol and 1 mL of toluene were added, and the mixture was refluxed overnight. Solvent was evaporated, and the crude washed with H_2O/methanol 1:1 (v/v). Finally, SubPc **3** was further purified, and its regioisomers separated through column chromatography in silica gel (hexane/toluene 2:3 (v/v)). Yield: 60%

RESULTS AND DISCUSSION

Synthesis of Building Blocks. The synthesis of SubPc **2** (Scheme 1) had been reported in 2008 with an overall yield of 35% starting from 4-iodophthalonitrile.[11] In this article, we describe an optimized version of this synthesis, which may be scaled up to gram quantities of the starting materials (Scheme 1). The first step of the synthetic route consists of condensation

Scheme 1. Synthesis of Precursor SubPc 2

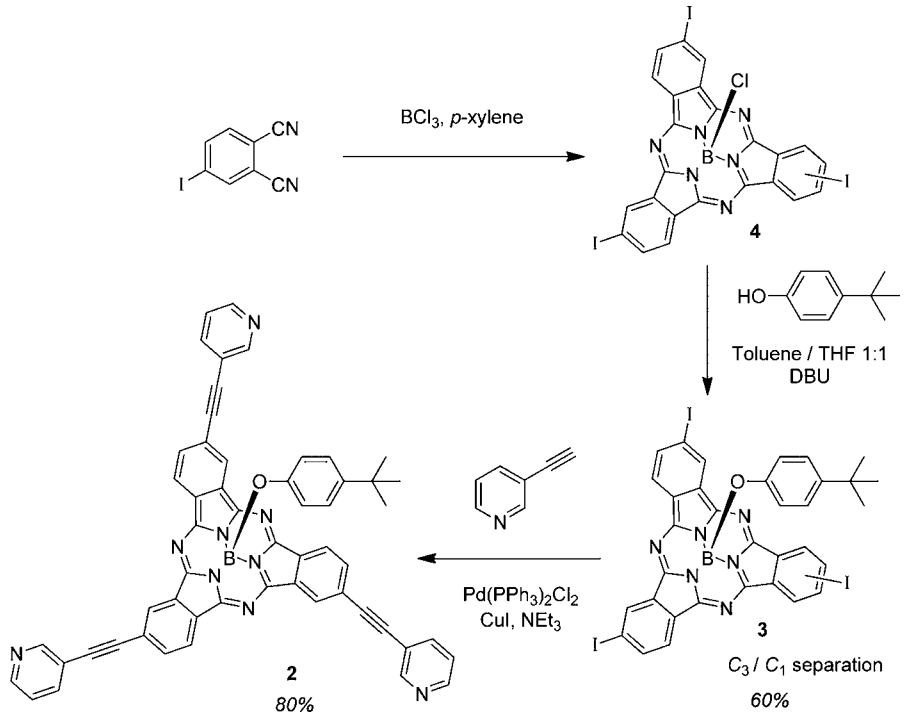

dx.doi.org/10.1021/ja404234n | J. Am. Chem. Soc. 2013, 135, 10503–10511

Scheme 2. Self-Assembly of SubPc-Based Metallosupramolecular Capsules 5a−d

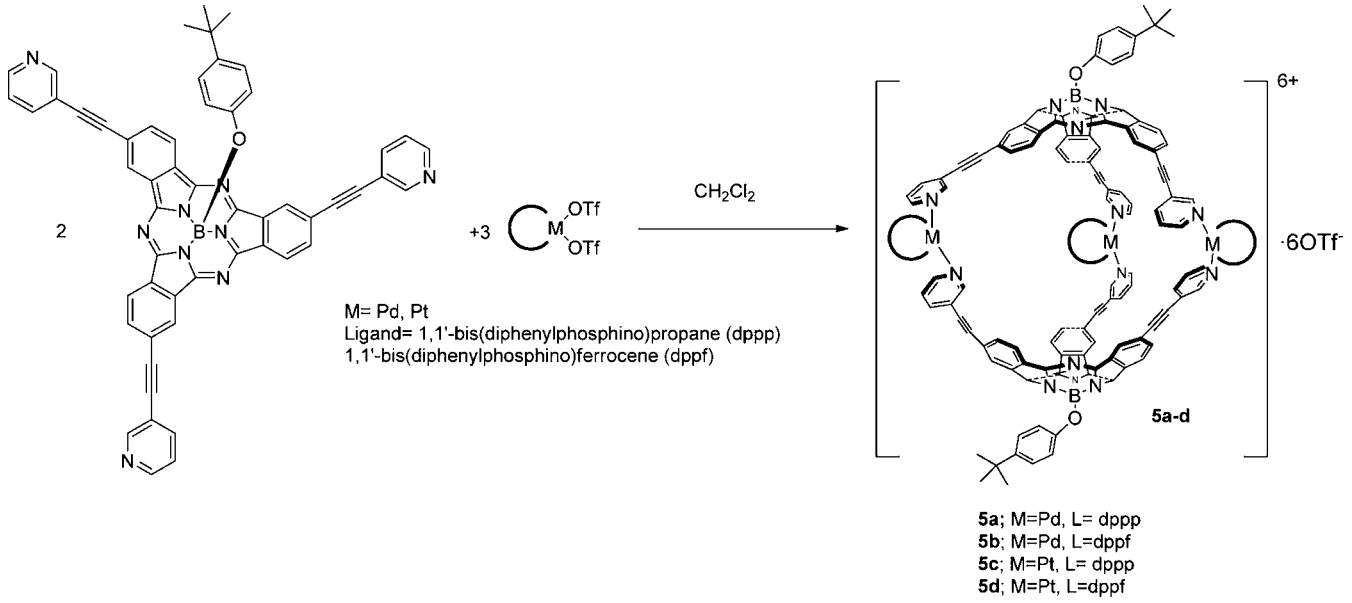

of 4-iodophthalonitrile in the presence of boron trichloride in refluxing *p*-xylene. The crude condensation product was directly treated with 2.5 equiv of 4-*t*-butylphenol in a 1:1 mixture of THF and toluene in the presence of a substoichiometric amount of DBU at reflux for 18−24 h to complete, in a one pot process, the substitution of the axial chlorine atom.[12] SubPc **3** was obtained in an overall yield of 60%. The 4-*t*-butylphenoxy group provides both solubility and stability to the macrocycle. C_3 and C_1 regioisomers of SubPc **3** were isolated by column chromatography on silica gel. Finally, the C_3 isomer of SubPc **3** was subjected to a triple Sonogashira cross coupling reaction with 3-ethynylpyridine in the presence of $PdCl_2(PPh_3)_2$ and copper iodide, affording the desired SubPc **2** in 80% yield. The overall yield of the synthetic route is 48%.

The synthesis of precursor metal complexes Pd(dppp)$(OTf)_2$, Pd(dppf)$(OTf)_2$, Pt(dppp)$(OTf)_2$, and Pt(dppf)$(OTf)_2$ was carried out following procedures described by Stang et al.[13]

SubPc-based capsules **5a−d** (Scheme 2) were obtained by treating the corresponding Pt or Pd acceptors with tritopic pyridyl ligand **2** in a 3:2 ratio in dichloromethane solution. The isolated yields for the self-assemblies are shown in Table 1.

Self-assembled capsules with dppp ligand were successfully obtained in quantitative yields. The low yields detected for **5b** and **5d** may be a consequence of the rigidity of both the SubPc and the ferrocene ligand, which, when combined, do not easily fulfill the required square-planar geometry of the metal. Higher yields for Pt compounds arise from the higher strength of the metal−nitrogen bonds.

All compounds were characterized by ^{1}H, ^{31}P, and ^{19}F-NMR, IR, UV−vis spectroscopies, and electrospray ionization mass spectrometry (ESI-MS). The most remarkable feature of the ^{1}H NMR spectra is the downfield shift of the proton in ortho position to the N of the pyridine due to the coordination of pyridine to the metal center. This signal appears at 9.01 ppm in the free SubPc and shifts up to 9.65 ppm in the case of capsules bearing dppp ligand. In the case of the dppf capsules, the downfield shift is not so prominent. ^{1}H NMR spectra also reveal more defined signals for the platinum capsules due to the less dynamic nature of the equilibria that are present in solution. In the case of **5b** and **5d**, bearing ferrocenyl secondary ligands, the loss of planar symmetry of the ferrocene moiety in the capsules gives rise to four signals. These results are consistent with the formation of the capsules.

Table 1. Yields of Self-Assembly for Capsules 5a−d[a]

	reaction time (h)	template	yield (%)
5a	24	−	>90[b]
5b	60	−	17[b]
5c	42	−	>90[b]
	18	−	28[c]
	18	C_{60}-PCBM	47[c]
	18	C_{70}-PCBM	53[c]
5d	72	−	25[b]
	18	−	11[c]
	18	C_{60}-PCBM	20[c]
	18	C_{70}-PCBM	89[c]

[a]Yields are listed for optimized reaction conditions (time) and reaction times in which equilibrium is not reached (in that cases, yields are indicated for self-assembly in the presence or absence of a guest (see Discussion section). [b]Optimized reaction conditions. [c]Equilibrium is not reached.

^{31}P NMR showed one singlet in all cases, accompanied by two ^{195}Pt satellites for **5c** and **5d**. The chemical shift of these singlets (Table 2) differs from those recorded for the original metal complexes and, in turn, corroborates that the chemical environment of P has changed after the self-assembly process.

ESI-MS further confirmed the self-assembly process. Peaks corresponding to $[M\text{-}2OTf]^{2+}$, $[M\text{-}3OTf]^{3+}$, and $[M\text{-}4OTf]^{4+}$ were found in the spectra of **5a** and **5c**. Mass spectra of capsules bearing ferrocene ligands did not yield any relevant results as far as the formation of the capsules is concerned. No signals corresponding to capsule compounds were found, most probably as a consequence of the lack of stability of these assemblies during the ionization process.

Host−Guest chemistry. The host−guest properties of our systems were also studied. First, ESI mass spectra of samples containing cage **5a** and different guests were recorded (Figure

dx.doi.org/10.1021/ja404234n | J. Am. Chem. Soc. 2013, 135, 10503−10511

Table 2. ^{31}P-NMR Chemical Shifts for Precursor Metal Complexes and Capsules 5a–d

	δ ^{31}P (ppm)	J_{Pt-P} (Hz)
$Pd(dppp)(OTf)_2$	7.70	–
$Pd(dppf)(H_2O)(OTf)_2$	46.17	–
$Pt(dppp)(OTf)_2$	−9.38	3886
$Pt(dppf)(H_2O)(OTf)_2$	15.81	3074
5a	6.23	–
5b	27.89	–
5c	−15.28	2988
5d	16.11	2988

2). The experiments included a variety of guests that could interact via $\pi-\pi$ stacking with the host and that present interest as potential electron or energy donors or acceptors. The guests were pentacene, ferrocene carboxylic acid, C_{60}, C_{70}, and C_{60}-PCBM ([6,6]-phenyl C_{61}butyric acid methyl ester).

Mass spectra corroborated the formation of complexes with fullerenes. In particular, peaks for the loss of two, three, and four counterions were found (Table 3), although the intensity of these signals was rather low. From these results we conclude that fullerenes are suitable guests for our SubPc-based capsules.

No encapsulation of pentacene was observed. On the other hand, ferrocene carboxylic acid provoked splitting of the capsule, due to the coordination of the carboxy group to Pd.

To confirm that the fullerene is present inside the capsule, we took advantage of template effect. In this regard, the self-assembly was carried out in the presence of soluble fullerene guests to probe the preorganization of SubPcs before they coordinate the metal centers. This preorganization would arise from interactions of the fullerenes with the concave face of SubPcs and would induce an increase of the yield. Hence, experimental conditions, in which the yield of self-assembly was not optimum, were chosen (18 h of reaction). The experimental procedure implied stirring first the SubPc and the guest together for 1h and subsequently adding the platinum complex. Notably, the expected increase in yields was observed with only 1.2 equiv of the guests (Table 1). Moreover, if the guest is not entirely removed during the work-up, the ^{1}H and ^{31}P NMR spectra show the same signals of the stoichiometric mixture of hosts and guests.

Table 3. Signals Observed in ESI-MS Experiments Corresponding to the Formation of Adducts of the Corresponding Guest with cage 5a (peaks observed, m/z)

	$[M\text{-}2OTf]^{2+}$	$[M\text{-}3OTf]^{3+}$	$[M\text{-}4OTf]^{4+}$
pentacene	–	–	–
ferrocene carboxylic acid	–	–	–
C_{60}	2282	1473	1067
C_{70}	–	1511	1097
C_{60}-PCBM	2344	1536	1115

Next, we examined the stoichiometry of the complexes and their binding constants. To this end, Job plot experiments (Figure 3) for cages **5c** and **5d** with C_{60}-PCBM were performed. Here, the absorption spectra were recorded in chloroform. No appreciable alterations were observed in the spectra, but subtraction of the theoretical absorbance of the capsule and the fullerene afforded ΔA values that were plotted versus the mole fraction of SubPc. These values gave rise to curves showing maxima at $\chi = 0.5$, which correlates with a 1:1 stoichiometry. In principle, the binding constants for 1:1 complexes might be directly derived from the Job plot[14] (Table 4). However, this method is rather inaccurate. Hence, NMR experiments were carried out in order to obtain more reliable values for the binding constants.

A titration of capsule **5c** with C_{60}-PCBM, which was followed by ^{1}H and ^{31}P NMR spectroscopy (Figures 4 and S1), indicates that the equilibrium is slow on the NMR time scale. Specifically, we observe signals that relate to the free cage and the complex. This fact is particularly pronounced for proton **a** (Figure 4) and in the signal of ^{31}P (Figure S1). As a consequence, we are able to calculate the binding constants directly from the ^{1}H and ^{31}P NMR spectra (Figures 4 and S1 and S2). The values obtained from the ^{1}H NMR spectra are shown in Table 4. The latter reveal that C_{70}-PCBM forms more stable associates with our capsules. A likely rationale implies its size, which seems more appropriate for the encapsulation. Furthermore, ^{1}H and ^{31}P NMR spectra give rise to a loss of symmetry regarding the capsule signals—three peaks are observed for each proton and phosphorus (Figure S2). From the latter we conclude that the guest has highly limited freedom inside the cage. Unfortunately, in the case of Pd cages, the equilibrium is faster, and no remarkable shift of any signal was

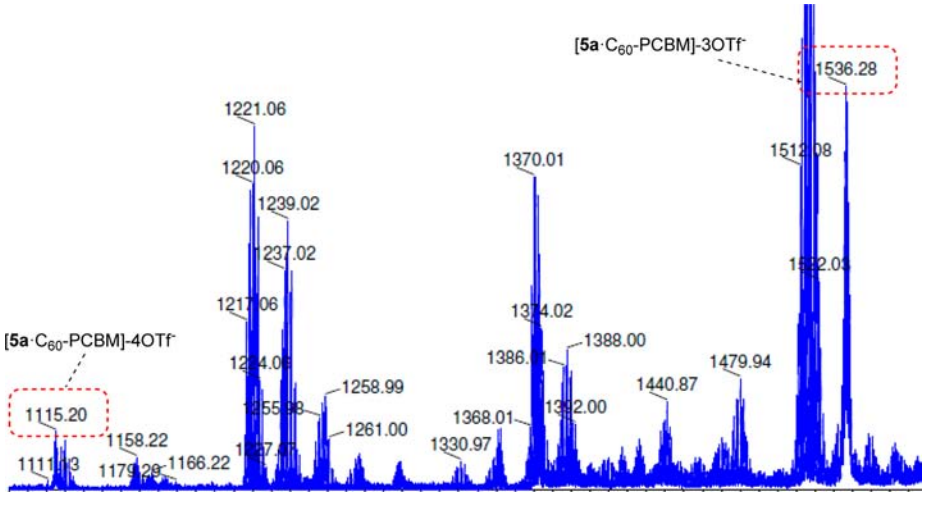

Figure 2. ESI-MS spectrum of cage **5a** with C_{60}-PCBM; signals corresponding to the supramolecular complex are indicated.

dx.doi.org/10.1021/ja404234n | J. Am. Chem. Soc. 2013, 135, 10503–10511

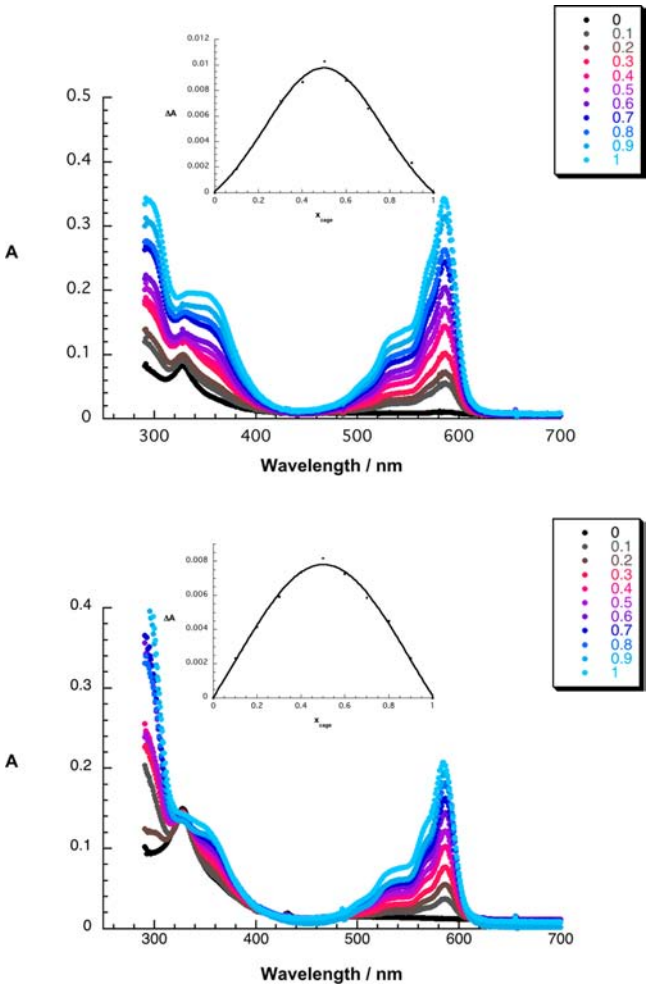

Figure 3. Absorption spectra recorded in chloroform during Job plot experiments of **5c** and C_{60}-PCBM (total concentration = 2×10^{-6} M, upper part) and **5d** and C_{60}-PCBM (total concentration = 3×10^{-6} M, lower part) at different mole fractions (see figure legend for details). Insets show the plot of ΔA (380 nm) vs mole fraction, with the maximum of the curves at 0.5, which indicates the 1:1 stoichiometry of the adducts.

observed upon addition of the guest. Hence, the binding constants could not be obtained from NMR experiments.

Photophysics. Photophysical studies of the cages were carried out to determine the impact of metal coordination as well as fullerene encapsulation on SubPc. In particular, fluorescence quantum yields of **5a–d** as well as that of the precursor SubPc **2** were determined by comparison with rhodamine 6G, which was chosen as standard.[15] We noted that the presence of both palladium and platinum quench the SubPc fluorescence, which was not that unexpected considering heavy-atom effects, etc. However, in the case of palladium, the quenching turned out to be appreciably stronger. Please note that metal–ligand charge transfer, that is, from platinum to the pyridine ligands, has been observed in related self-assembled triangles and squares.[16] Despite the fact that we have no sound evidence for a similar behavior taking place in our systems, it is, nevertheless, likely to assist in explaining why Pd deactivates more strongly the fluorescence of SubPcs.

Subsequently, the cages were titrated with different guests. In any of the titrations, fluorescence spectroscopy was employed to monitor the changes. In general, the platinum-containing cages gave rise to a weak SubPc fluorescence quenching upon addition of the guests. Nevertheless, we were able to derive binding constants of about 10^4 M^{-1} (Figure 5 and Table 4).

Despite the weak fluorescence quenching, several interesting trends emerged. For example, comparing the different cages, fluorescence quenching was only observed when Pt is incorporated. Overall, this is not surprising considering that the presence of palladium causes a strong decrease of the SubPc fluorescence quantum yields. Regarding the guests, pristine C_{60} seems to interact more strongly than its derivative. A likely explanation infers the disruption of $\pi-\pi$ stacking caused by the substituent on the fullerene. C_{70}-PCBM, on the other hand, showed higher binding constants than C_{60}-PCBM—a finding that is in good agreement with the NMR results. Finally, comparing the same guests in different solvents revealed that a stronger fluorescence quenching occurs in CH_2Cl_2 than in toluene. The origin of the latter implies a better desolvation of the fullerenes in CH_2Cl_2.

To examine the excited-state interactions between the SubPc cages and encapsulated C_{60}, we turned to pump probe measurements with C_{60}·**5c** and C_{60}·**5d.** First, we studied, however, C_{60} and SubPc **2**. As a matter of fact, the differential absorption spectra, taken right after the excitation of C_{60} at 420 nm, respectively, show the instantaneous transformation, ~1 ps, of high-lying singlet excited states into the lowest vibrational state of the singlet excited state of C_{60} (Figure S3). In particular, marked transitions develop in the near-infrared region with maxima at 960 nm for C_{60}. This singlet excited state (1.9 eV) deactivates slowly, 1.5 ± 0.1 ns, via intersystem crossing to the energetically lower lying triplet excited state (1.52 eV). Notably, the lifetime of intersystem crossing was determined from multiwavelength analyses. A newly developing band at 750 nm reflects the diagnostic signature of the triplet excited state of C_{60}. Upon 540 nm excitation of SubPc **2** (Figure 6), its singlet excited state (2.1 eV) evolves, whose spectral characteristics include transient maxima at 460, 485, 640, 665, and 760 nm as well as transient bleaching between

Table 4. Binding Constants (M^{-1}) Calculated for Capsules 5a–d and C_{60}, C_{60}-PCBM, or C_{70}-PCBM with All the Techniques Discussed in the Text

	Job plot[a]		^{1}H NMR[a]		fluorescence quenching			
	5c	**5d**	**5c**	**5d**	**2**	**5a**	**5c**	**5d**
C_{60}-PCBM	1.2×10^4	7.7×10^3	4.6×10^4	3.2×10^2				
C_{70}-PCBM			1.5×10^5	2.2×10^3			4.57×10^{4b}	6.15×10^{4b}
C_{60}					[e,c]	[e,c,e,d]	$3.01 \times 10^{4c,e,d}$	

[a]Solvent $CHCl_3$. [b]Solvent CH_2Cl_2. [c]Solvent toluene. [d]Solvent toluene/MeCN 1:1 (v/v). [e]Fluorescence quenching was observed but the data could not be fit to obtain K_{eq}. Maximum quenching (lowest I/I_0) observed were the following: 0.92 (**2** + C_{60}), 0.94 (**5a** + C_{60}, toluene), 0.88 (**5a** + C_{60}, toluene/MeCN 1:1 (v/v)), 0.76 (**5c** + C_{60}, toluene/MeCN 1:1 (v/v)).

dx.doi.org/10.1021/ja404234n | J. Am. Chem. Soc. 2013, 135, 10503–10511

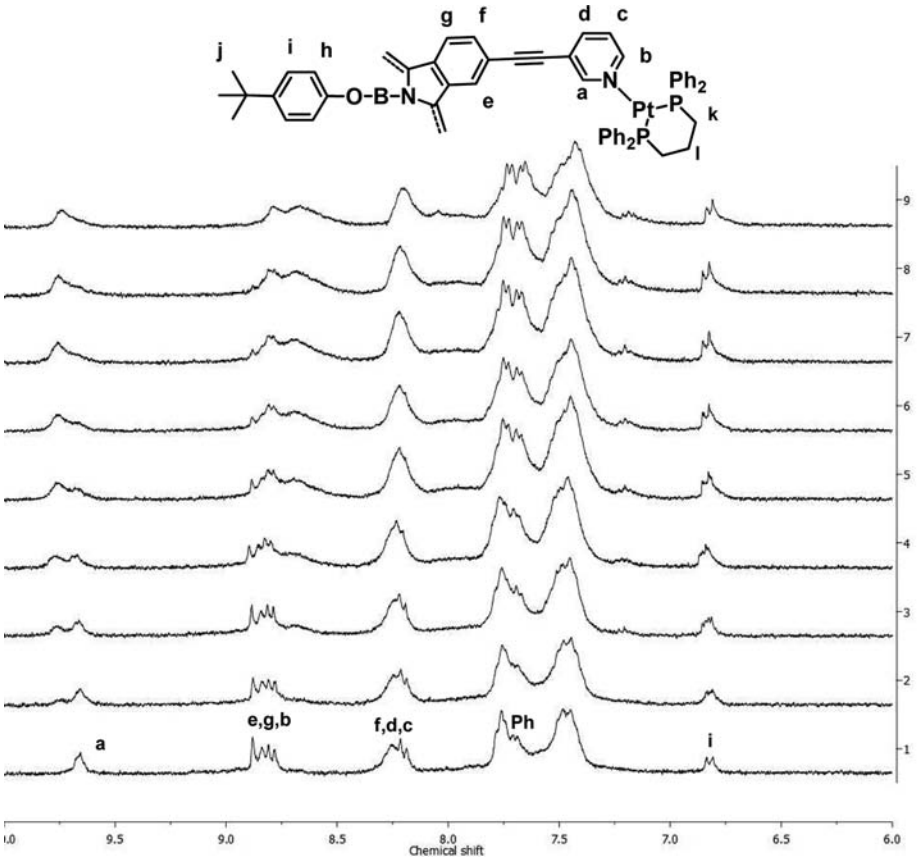

Figure 4. ^{1}H NMR spectra of a chloroform solution of **5c** (1.3×10^{-3} M) with variable concentrations of C_{60}-PCBM (from the bottom to the top, 0, 1.3×10^{-4}, 3.96×10^{-4}, 6.6×10^{-4}, 9.24×10^{-4}, 1.06×10^{-3}, 1.2×10^{-3}, 1.3×10^{-3}, 3.9×10^{-3} M). The assignation of protons is shown in the spectra of **5c** alone.

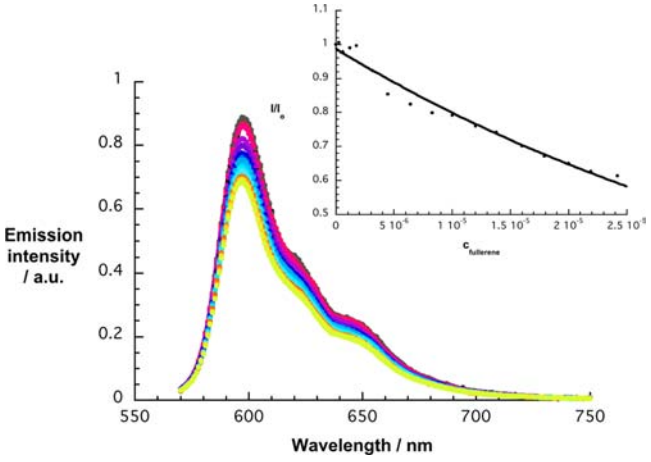

Figure 5. Emission spectra upon 550 nm excitation of a toluene solution of **5c** (5×10^{-6} M) with variable concentrations of C_{60} (0, 2.3×10^{-7}, 6×10^{-7}, 1.2×10^{-6}, 1.8×10^{-6}, 3.1×10^{-6}, 4.4×10^{-6}, 6.4×10^{-6}, 8.3×10^{-6}, 1.0×10^{-5}, 1.2×10^{-5}, 1.4×10^{-5}, 1.6×10^{-5}, 1.8×10^{-5}, 2×10^{-5}, 2.2×10^{-5}, 2.4×10^{-5} M). Inset shows the binding isotherm.

510 and 610 nm. The latter features a minimum at 590 nm. From multiwavelength analyses a singlet excited-state lifetime of 2.05 ± 0.1 ns was determined for **2**. For the correspondingly formed triplet excited state (1.45 eV) the most important spectroscopic feature is a 490 nm maximum.

Next, we performed experiments with SubPc cages **5d** and **5c** (Figures 7 and S4), which were like SubPc **2** photoexcited at 540 nm. Similar to what is seen for SubPc **2**, photoexcitation results in the formation of SubPc centered singlet excited states. In particular, 465, 485, 640, 660, and 760 nm maxima as well as 460, 485, 640, 670, and 760 nm maxima evolve for SubPc cages **5d** and **5c**, respectively, next to a minimum for both at 590 nm. In comparison to **2**, the presence of platinum exerts, however, in **5d** and **5c** an acceleration of the singlet excited-state decay, 1.1 ± 0.1 ns for **5d** and 1.2 ± 0.2 ns for **5c**, without yielding, however, a different photoproduct. Here, it is again the triplet excited state that is discernible by means of the 490 nm marker. But it is only the platinum that seems active, while ferrocene, which is present in **5d**, lacks any appreciable impact in neither a kinetic nor a spectroscopic sense.

Finally, SubPc cages **5d** and **5c** were treated with 1, 2, 5, 6, and 8 equiv of C_{60} to yield C_{60}·**5d** and C_{60}·**5c**, respectively, and subjected to pump−probe experiments (Figures 8 and S5). In sharp contrast to SubPc **2** as well as to SubPc cages **5d** and **5c**, **5d** and **5c** give rise upon 540 nm excitation in the presence of different equivalents of C_{60} to a fast deactivation, 2 ± 1 ps for **5d** and 3 ± 1 ps for **5c**, of the SubPc singlet excited state. Simultaneous to the rapid decay in the visible, the C_{60} singlet−singlet features grow in in the near-infrared, revealing identical dynamics. From this we conclude the transduction of singlet excited-state energy to yield the C_{60} singlet excited state. In C_{60}, intersystem crossing, 1.5 ± 0.1 ns, to the energetically lower lying C_{60} triplet dominates the deactivation of the singlet excited state, *vide supra*. In C_{60}·**5d** and C_{60}·**5c** the 960 nm

dx.doi.org/10.1021/ja404234n | J. Am. Chem. Soc. 2013, 135, 10503−10511

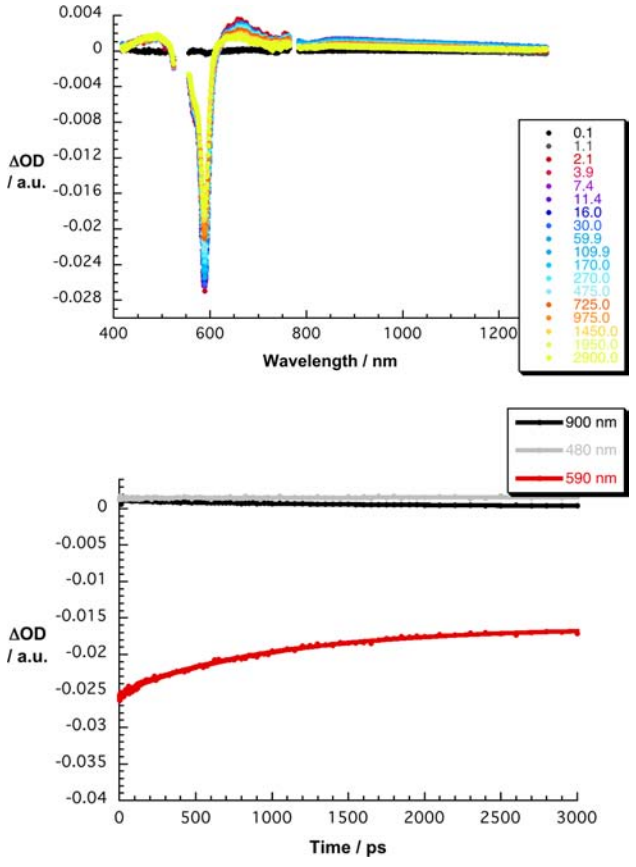

Figure 6. Upper part: differential absorption spectra (visible and near-infrared) obtained upon femtosecond pump−probe experiments (540 nm) of SubPc **2** (8.3×10^{-5} M) in toluene with several time delays between 0.1 and 2800 ps at room temperature (see figure legend for details). Lower part: time absorption profiles at 900 (black), 480 (light gray), and 590 (red) nm monitoring the excited-state dynamics.

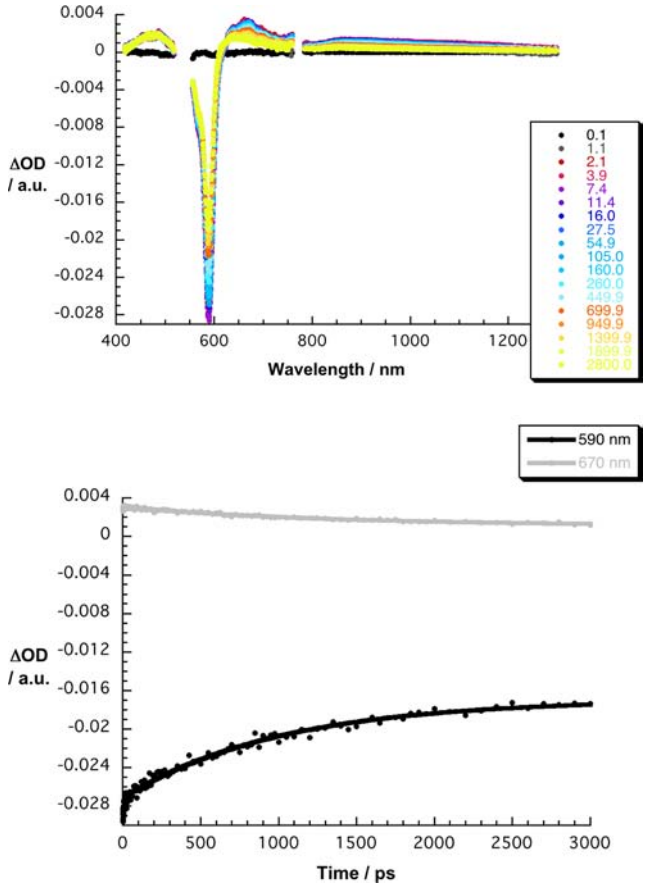

Figure 7. Upper part: differential absorption spectra (visible and near-infrared) obtained upon femtosecond pump probe experiments (540 nm) of **5c** (1.3×10^{-5} M) in toluene with several time delays between 0.1 and 2800 ps at room temperature (see figure legend for details). Lower part: time absorption profiles at 590 (black) and 670 (light gray) nm monitoring the excited-state dynamics.

transition product of the initial transfer of singlet excited-state energy decays with kinetics, which are barely faster. In fact, the lifetimes are 1.4 ± 0.1 ns for C_{60}·**5d** and C_{60}·**5c**. Interesting is, however, that we did not find the characteristic C_{60} triplet features that is a strong triplet−triplet transition at 750 nm, at the end of the C_{60} singlet excited-state deactivation. Instead, a maximum around 490 nm and a minimum at 590 nm were concluded. The latter are excellent matches of the SubPc triplet excited state, *vide supra*. From this we infer that the C_{60} triplet excited state (1.52 eV), once formed, undergoes a thermodynamically allowed transfer of triplet energy to the SubPc (1.45 eV). Nearly similar kinetics at the 590 nm minimum, which allowed us to follow the generation of the SubPc triplet, further furnishes the following kinetic assignment. The rate determining and, in turn, the slower step in the SubPc triplet formation is the C_{60} intersystem crossing.

■ CONCLUSIONS

In the current work, four different SubPc-based capsules were newly prepared, and their host−guest properties with a number of fullerenes were explored. In a wide plethora of experiments, the ability of these SubPc-based capsules to encapsulate pristine fullerenes and fullerene derivatives was unambiguously confirmed. In this context, preorganization of SubPc **2** by means of coordinating metal centers leads to binding constants that are similar to those previously observed for non-preorganized electron donating SubPcs.[6]

In terms of binding modes, NMR investigations were decisive. The use of mixtures containing equimolar concentrations of hosts and guests enabled direct calculations of the corresponding binding constants. As a matter of fact the binding constants were also estimated on the basis of fluorescence titration assays. In the latter the fluorescence quenching of the capsules was monitored as a function of encapsulated fullerene guests. Quite interesting is the fact that the binding constants attest stronger interactions of the capsules with C_{70} than with C_{60}.

Finally, time-resolved photophysical investigations were performed to shed light onto the nature of the host−guest interactions. In fact, pump probe experiments corroborated that photoexcitation of the different SubPc-based capsules is the inception to a rapid transduction of singlet excited-state energy to the encapsulated fullerene guests. Once completed, the latter is subject to an intersystem crossing before the energy is being back transferred to the SubPc-based capsules. Here, it is, however, a slow transduction of triplet excited-state energy. The corresponding triplet excited state deactivates eventually to the electronic ground state.

dx.doi.org/10.1021/ja404234n | J. Am. Chem. Soc. 2013, 135, 10503−10511

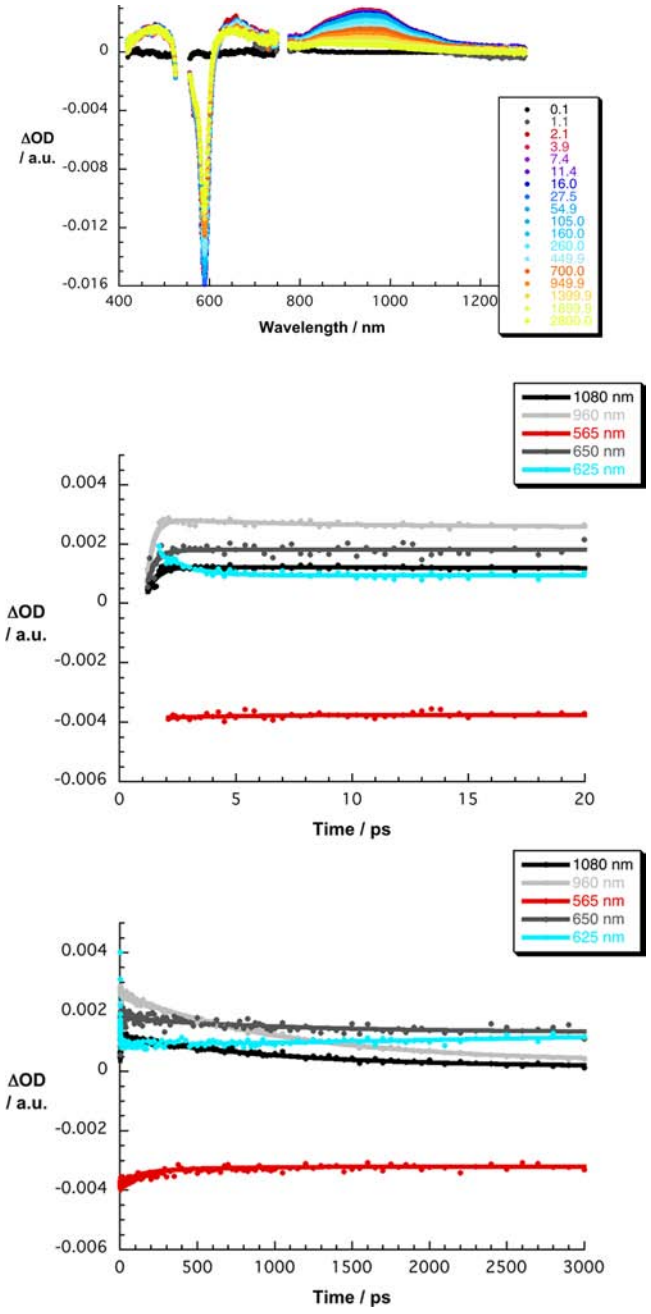

Figure 8. Upper part: differential absorption spectra (visible and near-infrared) obtained upon femtosecond pump probe experiments (540 nm) of **5d** (1.3×10^{-5} M) with 2 eq of C_{60} in toluene with several time delays between 0.1 and 2800 ps at room temperature (see figure legend for details). Central and lower part: time absorption profiles at **5d** (central) and C_{60}·**5d** (lower) at 1080 (black), 960 (light gray), 565 (red), 650 (dark gray), and 625 (light blue) nm monitoring the excited-state dynamics.

■ ASSOCIATED CONTENT

Ⓢ Supporting Information

Analytical and electrochemical data of compounds **5a–d**, details for titrations and Job plots, and additional transient spectra. This material is available free of charge via the Internet at http://pubs.acs.org.

■ AUTHOR INFORMATION

Corresponding Author

tomas.torres@uam.es; christian.claessens@uam.es; dirk.guldi@fau.de

Notes

The authors declare no competing financial interest.

■ ACKNOWLEDGMENTS

Support is acknowledged from the Spanish MICINN (CTQ2011-24187/BQU and CONSOLIDER INGENIO 2010, CSD2007-00010 on Molecular Nanoscience), the Comunidad de Madrid (MADRISOLAR-2, S2009/PPQ/1533), the EU (FP7- ICT-2011.3.6, Nr: 287818), Fonds der Chemischen Industrie (FCI) and Deutsche Forschungsgemeinschaft (SFB 583), and the "Solar Technologies Go Hybrid" initative by the state of Bavaria.

■ REFERENCES

(1) Claessens, C. G.; González-Rodríguez, D.; Torres, T. *Chem. Rev.* **2002**, *102*, 835–853. Torres, T. *Angew. Chem., Int. Ed.* **2006**, *45*, 2834–2837.

(2) (a) Pérez, E. M.; Martín, N. *Chem. Soc. Rev.* **2008**, *37*, 1512–1519. (b) Canevet, D. C.; Pérez, E. M.; Martín, N. *Angew. Chem., Int. Ed.* **2011**, *50*, 9248–9259.

(3) (a) del Rey, B.; Keller, U.; Torres, T.; Rojo, G.; Agulló-López, F.; Nonell, S.; Martí, C.; Brasselet, S.; Ledoux, I.; Zyss, J. *J. Am. Chem. Soc.* **1998**, *120*, 12808–12817. (b) Medina, A.; Claessens, C. G.; Rahman, G. M. A.; Lamsabhi, A. M.; Mó, O.; Yáñez, M.; Guldi, D. M.; Torres, T. *Chem. Commun.* **2008**, *15*, 1759–1761. (c) González-Rodríguez, D.; Torres, T.; Olmstead, M. M.; Rivera, J.; Herranz, M. A.; Echegoyen, L.; Atienza, C.; Guldi, D. M. *J. Am. Chem. Soc.* **2006**, *128*, 10680–10681. (d) Rodríguez-Morgade, M. S.; Claessens, C. G.; Medina, A.; González-Rodríguez, D.; Gutiérrez-Puebla, E.; Monge, A.; Alkorta, I.; Elguero, J.; Torres, T. *Chem.—Eur. J.* **2008**, *14*, 1342–1350. (e) Camerel, F.; Ulrich, G.; Retailleau, P.; Ziessel, R. *Angew. Chem., Int. Ed.* **2008**, *46*, 9008–9012. (f) El-Khouly, M. E.; Shim, S. H.; Araki, Y.; Ito, O.; Kay, K.-Y. *J. Phys. Chem. B* **2008**, *112*, 3910–3917. (g) El-Khouly, M. E.; Ju, D. K.; Kay, K.-Y.; D'Souza, F.; Fukuzumi, S. *Angew. Chem., Int. Ed.* **2010**, *21*, 6193–6202. Caballero, E.; Fernández-Ariza, J.; Lynch, V. M.; Romero-Nieto, C.; Rodríguez-Morgade, M. S.; Sessler, J. L.; Guldi, D. M.; Torres, T. *Angew. Chem., Int. Ed.* **2012**, *51*, 11337–11342.

(4) González-Rodríguez, D.; Torres, T.; Guldi, D. M.; Rivera, J.; Herranz, M. A.; Echegoyen, L. *J. Am. Chem. Soc.* **2004**, *126*, 6301–6313.

(5) González-Rodríguez, D.; Carbonell, E.; de Miguel Rojas, G.; Atienza Castellanos, C.; Guldi, D. M.; Torres, T. *J. Am. Chem. Soc.* **2010**, *132*, 16488–16500.

(6) Sánchez-Molina, I.; Claessens, C. G.; Grimm, B.; Guldi, D. M.; Torres, T. *Chem. Sci.* **2013**, *4*, 1338–1344.

(7) (a) Ziessel, R.; Ulrich, G.; Elliott, K. J.; Harriman, A. *Chem.—Eur. J.* **2009**, *15*, 4980–4984. (b) Shimizu, S.; Nakano, S.; Hosoya, T.; Kobayashi, N. *Chem. Commun.* **2011**, *47*, 316–318.

(8) (a) Chakrabarty, R.; Mukherjee, P. S.; Stang, P. J. *Chem. Rev.* **2011**, *111*, 6810–6918. (b) Sun, Q.-F.; Murase, T.; Sato, S.; Fujita, M. *Angew. Chem., Int. Ed.* **2011**, *50*, 10318–10321. (c) Mugridge, J. S.; Bergman, R. G.; Raymond, K. N. *J. Am. Chem. Soc.* **2011**, *133*, 11205–11212. (d) Brusilowskij, B.; Dzyuba, E. V.; Troff, R. W.; Schalley, C. A. *Dalton Trans.* **2011**, *40*, 12089–12096. (e) Mal, P.; Breiner, B.; Rissanen, K.; Nitschke, J. R. *Science* **2009**, *324*, 1697–1699.

(9) Claessens, C. G.; Torres, T. *J. Am. Chem. Soc.* **2002**, *124*, 14522–1452.

(10) Claessens, C. G.; Torres, T. *Chem. Commun.* **2004**, 1298–1299.

(11) (a) Claessens, C. G.; Vicente-Arana, M. J.; Torres, T. *Chem. Commun.* **2008**, 6378–6380. (b) Claessens, C. G.; Sanchez-Molina, I.; Torres, T. *Supramol. Chem.* **2009**, *21*, 44–47.

(12) Claessens, C. G.; Gonzalez-Rodriguez, D.; del Rey, B.; Torres, T.; Mark, G.; Schuchmann, H.-P.; von Sonntag, C.; MacDonald, J. G.; Nohr, R. S. *Eur. J. Org. Chem.* **2003**, *14*, 2547−2551.
(13) (a) Cao, D. H.; Saito, S.; Arif, A. M.; Stang, P. J. *J. Am. Chem. Soc.* **1995**, *117*, 6273−6283. (b) Olenyuc, B.; Fan, J.; Arif, A. M.; Stang, P. J. *Organometallics* **1996**, *15*, 904−908.
(14) Bruneau, E.; Lavabre, D.; Levy, G.; Micheau, J. C. *J. Chem. Educ.* **1992**, *69*, 833−837.
(15) Kubin, R. F.; Fletcher, A. N. *J. Lumin.* **1982**, *27*, 455−462.
(16) Flynn, D. C.; Ramakrishna, G.; Yang, H.-B.; Northrop, B. H.; Stang, P. J. *J. Am. Chem. Soc.* **2010**, *132*, 1348−1358.